



# Experiments and FE simulation for twin screw mixing of nanocomposite of polypropylene/multi-walled carbon nanotubes



H. Djoudi<sup>1</sup>, J.-C. Gelin<sup>2</sup>, T. Barrière<sup>\*</sup>

FEMTO-ST Institute, Applied Mechanic Laboratory, 24 rue de l'épithaphe, Besançon, France

## ARTICLE INFO

### Article history:

Received 1 November 2014

Received in revised form 22 December 2014

Accepted 28 December 2014

Available online 2 January 2015

### Keywords:

A. Carbon nanotubes

Particle-reinforced composites

B. Non-linear behavior

C. Modeling

Computational mechanics

## ABSTRACT

Elaboration of the feedstock in polymer/carbon nanotubes is introduced in both aspects of the experiments by a twin screw mixer, and the corresponded simulation of mixing process. The viscous behaviors are calibrated by a capillary rheometer under different temperature. The achieved data are used to determine the parameters in the suitable viscous laws with the satisfied verification. Front cover of the mixer is replaced by a transparent one, which permits the direct observation of mixing process, and the record of temperature evolution by an infrared camera with high performance IR imaging. The simulations of mixing processes in a twin screw mixer, with the determined viscous law and the temperature conditions justified by experiments, are realized by software COMSOL® with its performance in coupling of the multi-physics. Different referential frames and ALE formulation are used for the counter rotations of two screws in mixing chamber. The mechanism of nanocomposite mixing in twin screw chamber is investigated with the achieved results. Comparison between the results of simulation and experiments proved the proposed methods and the prepared feedstock for nanocomposite.

© 2015 Elsevier Ltd. All rights reserved.

## 1. Introduction

The development and improvement of nanocomposites will be a key advance in the future. Since the discovery of carbon nanotubes in 1991 by Iijima [1], the research in nanomaterial became one of the most promising fields. Carbon nanotubes (CNTs) are allotropes of carbon with cylindrical nanostructure. Their diameters range from one to ten nanometers, and lengths in the micrometer range as reported by Pötschke [2]. The analyses and experiments revealed that carbon nanotubes have excellent mechanical properties, with Young's modulus of individual CNT in TPa order and a tensile strength as high as 200 GPa as reported [3–5]. The measurement on multi-walled carbon nanotube (MWCNT) by Demczyk et al. [6] estimated that the elastic modulus is about 0.8 TPa with error eq. 1.14%. Due to the super mechanical properties and large potentials, important researches have been carried to develop various nanocomposites of polymer/carbon nanotubes by injection molding process. Shaffer et al. [7] set up the first reinforcement of nanotubes in polymeric based composites in 1999. Prashanthaa et al. assessed the rheological and

mechanical properties of polypropylene/MWCNT composites [8]. Lee et al. investigated their rheological and electrical properties [9].

The application of carbon nanotube based nanocomposites is not yet exhibited in practice, because of the uncertain load transfer between the matrix and the fibers. The homogeneous particles distribution and proper interfacial adhesion are crucial for successful preparation of the nanocomposites, as shown by Zhan et al. [10]. Thiébaud et al. [11] reported that the shear mixing by melt processing is currently one of the most used methods. They realized the simulation of mixing process in a twin screw mixer restricted in 2D model. Actually most studies are related to experiments, this work is aimed to provide a numerical counterpart. 3D Simulation of loaded polymer flows in a twin screw-mixer has been realized by finite elements method.

The elaboration of PP/MWCNT nanocomposites by a twin screw mixer is first introduced. Rheological characterization of PP/MWCNT elaborated samples at 4 selected temperatures (180, 200, 220 and 240 °C) has been conducted by a capillary rheometer, as reported [12]. These rheological properties are used to identify the viscosity parameters of flow models. Cross et al. [13] and Bourgeat et al. [14] suggested the way to fit the flow properties of polymers melt or a polymer solution by non-Newtonian flow model, i.e. to modify Newton's model by a variable viscosity that depends on the share rate and temperature. In order to characterize the flow of polymer/carbon nanotubes, the Carreau–Yasuda law has been adopted.

<sup>\*</sup> Corresponding author. Tel.: +33 3 81 66 60 75; fax: +33 3 81 66 67 00.

E-mail addresses: [hamza.djoudi@hotmail.fr](mailto:hamza.djoudi@hotmail.fr) (H. Djoudi), [jean-claude.gelin@univ-fcomte.fr](mailto:jean-claude.gelin@univ-fcomte.fr) (J.-C. Gelin), [thierry.barriere@univ-fcomte.fr](mailto:thierry.barriere@univ-fcomte.fr) (T. Barrière).

<sup>1</sup> Tel.: +33 3 81 66 60 10.

<sup>2</sup> Tel.: +33 3 81 66 60 35.

The second part involves the analysis and simulation of loaded polymer flows in mixing process by finite element method. COMSOL® multiphysics modeling software was used because of its efficiency for coupling of the multiphysics, the availability to add solution of the partial differential equations, and the convenience to cooperate with Matlab®. Evolution of the velocity fields, related shear rates, temperature fields and mixing torques during the mixing stage have been analyzed.

## 2. Experimental process

### 2.1. Elaboration of the nanocomposites

Nanocomposites of polypropylene (PP)/multi walled carbon nanotubes (MWCNTs) have been elaborated by mixing PP pellets [PP\_Sabic® PHC 31\_81, melt flow index 12.6 kg/10 min at 200 °C] with the masterbatch MWCNT produced by Chemical Vapor Deposition [NC7000 supplied by Nanocyl®, Belgium]. In order to properly disperse MWCNT in the polypropylene matrix, the chlorosulfonic acid and ultrasonication were used to get the carbon nanotubes dispersed properly. The acid adds positive charges to the surface of the nanotubes without damaging them, and causes the nanotubes to spontaneously separate from each other in their natural bundled form.

The mixing process was realized in a co-rotating twin screw mixer [Plastograph 50 W EHT] shown in Fig. 1. This equipment represents the upper capacity for velocity 150 rpm, temperature 500 °C, torque 200 N m, and volume 40 cm<sup>3</sup>. The Choice of optimal mixing condition follows the research realized in laboratory [15]. Duration of the mixing is 100 min, with a chamber temperature 200 °C, and a screw speed 60 rpm. The speed ratio between two screws is about 2:3. The left screw rotates clockwise while the right one rotates counterclockwise. Counter-rotation at different speeds provides proper compounding and mixing of the nanocomposites. Evolutions of the mixing torque and temperature have been measured by sensors in real time. A transparent front wall is used for the twin screw mixer in experiments. Evolution of the

temperature in cavity of the twin-screw mixer can be measured by an infrared camera of high thermal imaging quality, see Fig. 1.

The thermoplastic polymer matrix is polypropylene (Sabic PHC 31\_81), with melting temperature 152 °C, density 0.905 g cm<sup>-3</sup>, specific heat 1800 J/kg K and thermal conductivity 0.2 W/m K. The reinforcement by MWCNT (NC 7000) is Nanocyl® 7000, with diameter 9.5 nm, length 1.5 µm, thermal conductivity 3000 W/m K, purity 90%.

4 nanocomposite samples of different MWCNT loadings in polypropylene matrix, 10%, 20%, 30% and 40% in weight, have been elaborated. For a reference, pure PP matrix has been squeezed with the same mixing parameters. Main challenge in elaboration of the nanocomposites is to get uniform and homogenous dispersion of the MWCNT in PP matrix. The mixing torque depends on shear viscosity of the loaded polymers as reported by Kong et al. [16]. Evolutions of the mixing torque for PP/MWCNT samples are measured, and compared later with the simulation results in Fig. 10. When PP/MWCNT compounds are fed into the mixer, very high torque values are measured due to their solid state. After 10 min, the PP gets into molten state then it results in decrease of the mixing torque. More MWCNTs amount in mixture results in larger mixing torque, because of the effect of long carbon nanotubes and the formation of MWNT network in polymer matrix.

### 2.2. Rheological characterization of PP/MWCNT nanocomposites

Rheological tests are the essential ways to identify a suitable viscosity model. The shear viscosity of PP/MWCNT nanocomposite has been measured for different MWCNT ratios, at different temperatures and different shear rates. A capillary rheometer provided by Malvern®, with a capillary die of diameter 1 mm and length 16 mm, has been used in the range of shear rate 10–10<sup>4</sup> s<sup>-1</sup>. The relationship between shear viscosity and shear rate for PP/MWCNT samples are obtained, and then used for calibration of the behavior model as shown in Fig. 5. The effect of temperature on shear viscosity is shown in Fig. 2.

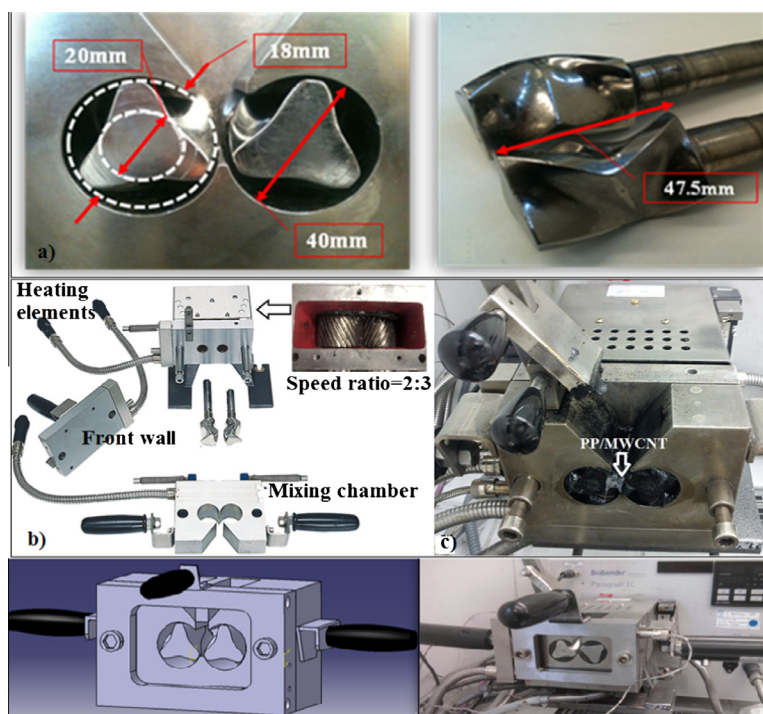


Fig. 1. Twin screw mixer Brabender® EC W50EHT: (a) mixing chamber and screws, (b) installation of the twin-screw mixer, (c) mixing process of the PP/MWCNT feedstock and (d) replacement of the front wall by a transparent one.

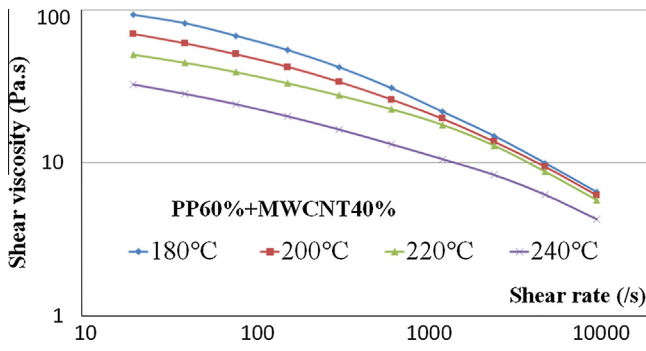


Fig. 2. Effect of the temperature on shear viscosity-shear rate relationship for 40 wt.% PP/MWCNT nanocomposite, under temperature 180, 200, 220 and 240 °C.

At temperature 200 °C, shear viscosity for pure PP and PP/MWCNT nanocomposites decreases when shear rate increases, as reported by Kellarakis et al. [17] and Gu et al. [18]. The PP/MWCNT nanocomposites exhibit a shear thinning effect whereas the pure PP exhibits small shear rate dependence for the range of shear rate ( $10\text{--}10^2\text{ s}^{-1}$ ). Higher than 240 °C, the PP viscosity curves exhibit much steeper slope at low shear rate. But for shear rate in the higher range  $10^2\text{--}10^4\text{ s}^{-1}$ , the flow behaviors of PP/MWCNT nanocomposites are practically the same as pure PP. The shear viscosity curves indicate clearly the different effects of MWCNTs ratio at different shear rate. At low shear rate the addition of MWCNT results in increase of the viscosity, but viscosity is less sensitive to addition of the MWCNT at higher shear rate.

Both PP and PP/MWCNT nanocomposites exhibit non-Newtonian behaviors. The measurement on PP/MWCNT loaded at 40 wt.% reveals the decrease of shear viscosity when temperature increases. The trends are the same for other PP/MWCNT nanocomposites because viscosity of the polypropylene decreases when temperature increases.

### 2.3. Measurement of temperature in experiments

In order to record evolution of the temperature in nanomaterial during mixing, an infrared camera with high performance IR imaging is used with the data processing by computer. The software allows processing the images from infrared camera at fast frame

rate, and provides estimation of the temperature at any point in the zone of measurement. For this purpose, front wall of the mixer is replaced by a glass one, as shown in Fig. 1.

Temperature field evolution in 40 wt.% loaded PP/MWCNT during mixing stage, captured by infrared camera, is shown in Fig. 3. Chamber of the mixer is first preheated to 200 °C as shown in Fig. 3a by different electric cartridges. In the observation by transparent front, some back wall of the chamber can be observed in red color, which indicates the maximum temperature, too. Then the nanocomposite is fed into the heated mixer at solid state, and becomes molten after a few seconds, as shown in Fig. 3b. The nanocomposite reaches the set temperature in 90 s. It guarantees the optimal mixing conditions for homogeneous dispersion of MWCNTs in polymeric matrix.

### 3. Rheological behavior of the PP/MWCNT nanocomposites

Viscous behavior of flow material in a wide range of shear rate is essential for solution of the Navier–Stokes equations. Characterization of the viscosity for PP/MWCNT mixtures is done by fitting the experimental data to one of the viscosity models, as reported by Akdogan et al. [19]. The following behavior laws provided by literatures can be considered:

$$\mu(T, \dot{\gamma}) = \mu_0 \dot{\gamma}^n \quad (1)$$

$$\mu(T, \dot{\gamma}) = \frac{\mu_0}{(1 + \lambda \dot{\gamma})^{1-n}} \quad (2)$$

$$\mu(T, \dot{\gamma}) = \mu_0 \left(1 + (\lambda \dot{\gamma})^a\right)^{\frac{n-1}{a}} \quad (3)$$

These 3 expressions are known as the modified Ostwald, Cross and Carreau laws, respectively, where  $\mu_0$  is the zero shear rate viscosity,  $\lambda$  is the time scale and  $n$  stands for the shear rate sensitivity,  $0 < n < 1$ ,  $a$  is the power index and  $\dot{\gamma}$  is the shear rate expressed as following:

$$\dot{\gamma} = (1/2 \bar{D} : \bar{D})^{1/2} \quad (4)$$

where  $\bar{D}$  is the deviatoric strain rate tensor. Identification of the parameters consists to fit a set of the measured values by the shear

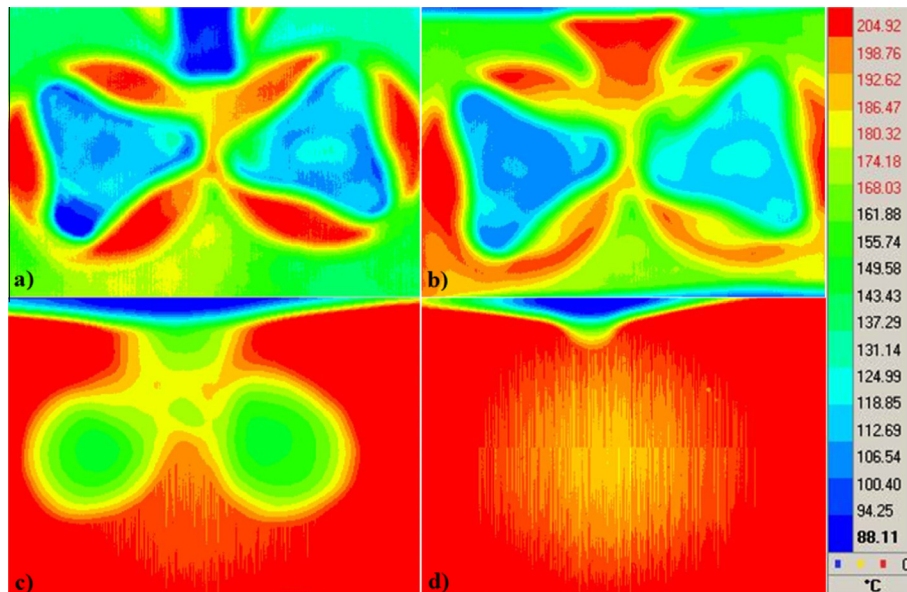


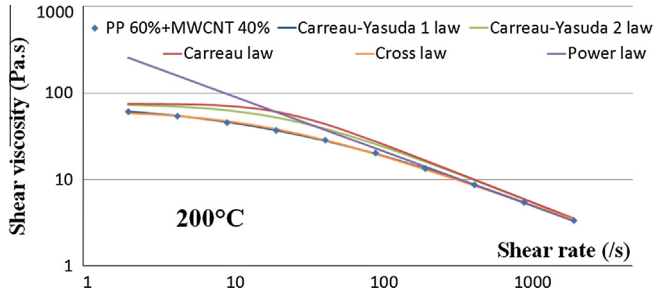
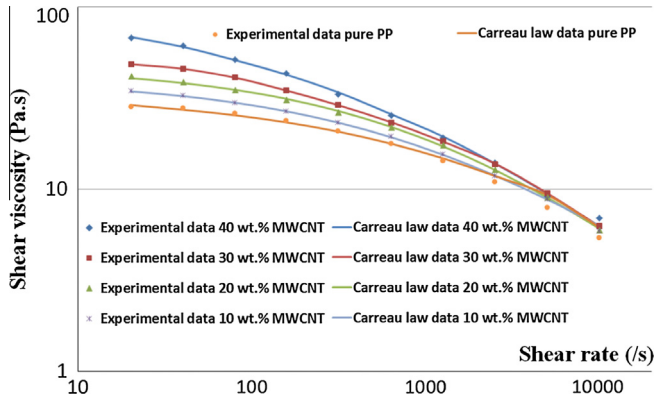
Fig. 3. Temperature fields measured from transparent front wall of the twin-screw mixer, for material 40 wt.% PP/MWCNT, mixer temperature 200 °C, rotation speed 30 rpm. (a) Before feeding of the material, (b) after 15 s, (c) after 60 s and (d) after 90 s.



**Table 1**

Identified parameters of viscosity models for the PP/MWCNT 40 wt.%.

	$T_{ref}$ (°C)	$\mu_0$ (Pa s)	$\lambda$ (s)	$n$	$a$	$b$
Ostwald	200	4e3	0.05	0.37		0.015
Cross	200	67.58	0.06	0.4	0.2	0.015
Carreau	200	74.97	0.0125	0.5	0.94	0.015
Carreau-Y1	200	68.02	0.03	0.45	0.2	0.015
Carreau-Y2	200	74.1	0.02	0.45	0.31	0.015

**Fig. 4.** Comparison among different flow models with the identified parameters in Table 1.**Fig. 5.** Shear viscosity versus shear rate measured at 200 °C for PP and different PP/MWCNT feedstock: experimental data and fitting curves of Carreau law.

viscosity curve that subjects to Cross or Carreau laws. Minimization of the difference between adopted model and experimental data results in the determination of parameters  $\mu_0$ ,  $\lambda$ ,  $a$  and  $n$ . Mathematically it is the solution of non-linear algebraic equations with 4 parameters. The viscosity represents a decreasing function of the temperature as reported by Fasina et al. [20]. A change in temperature  $\Delta T$  does not affect the functional dependence of  $\mu$  on  $\dot{\gamma}$ , but alters the zero shear viscosity and the shear rate at which transition from Newtonian to pseudo-plastic behavior occurs. The viscosity of polymer melts varies with temperature, according to the exponential relationship of Arrhenius:

$$\mu_0(T) = \mu_0 e^{-b\Delta T} \quad (5)$$

where  $b$  is the temperature sensitivity coefficient, its value ranges from 0.01 to 0.1 °C<sup>-1</sup>.

Ostwald law described in Eq. (1) is essentially a phenomenological description of fluid behavior in some range of the shear rate. In one sets  $a = 1$  in Eq. (3) Carreau–Yasuda law becomes the Cross law in Eq. (2). These laws appear to be a good compromise between the number of parameters and the measured experimental data.

Carreau–Yasuda viscosity law is commonly used for polymers and loaded polymers. The parameters  $\mu_0$ ,  $\lambda$ ,  $a$ ,  $b$  and  $n$  summarized in Table 1, have been identified for each behavior law by the solution of an inverse problem. Comparison among different behavior laws for PP/MWCNT nanocomposite with 40 wt.% MWCNT at 200 °C is shown in Fig. 4. The most accurate one is the Carreau–Yasuda 1 ( $a = 0.64$ ), it is retained for numerical simulation.

Relationship between the measured data and the identified Carreau–Yasuda law for pure PP and different PP/MWCNT nanocomposites is shown in Fig. 5. It exhibits a good agreement.

#### 4. Numerical simulation for mixing stage of PP/MWCNT nanocomposite

A 3D modeling and simulation of the PP/MWCNT nanocomposite flow in a co-rotating mixer has been realized by COMSOL® software. Carreau–Yasuda model is retained for flow behavior of the material. In order to take into account the rotations of two screws at different speeds, the domain of material flow is divided into three sub-domains as described in Fig. 6.

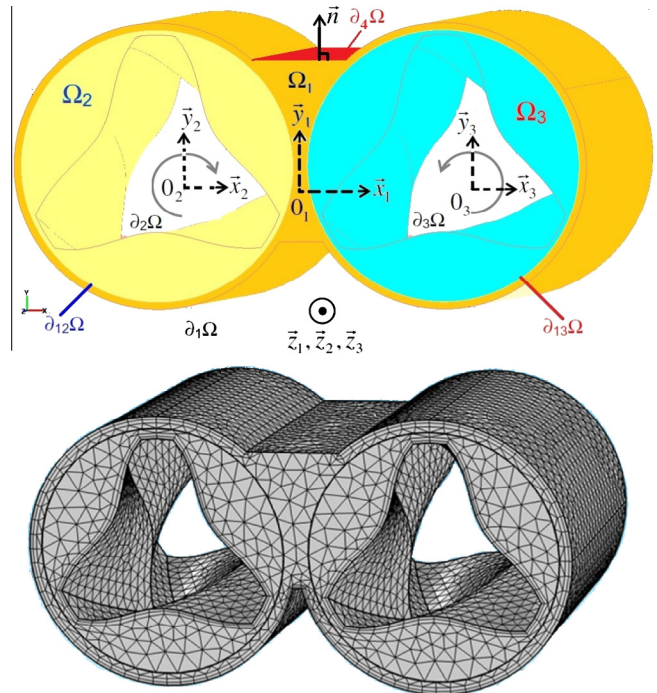
##### 4.1. Governing equations

For mixing stage of PP/MWCNT, the flow motion in subdomains  $\Omega_{1 \cup 2 \cup 3}$  is governed by Navier–Stokes equation and incompressibility condition, where  $\Omega_1$  is the outer subdomain and  $\Omega_{2 \cup 3}$  the inner subdomains. Under ALE description these equations are written as

$$\rho \left( \frac{\partial \mathbf{v}}{\partial t} + (\mathbf{v} - \mathbf{w}) \cdot \nabla \mathbf{v} \right) = -\nabla P + \mu(\dot{\gamma}, T) \Delta \mathbf{v} + \mathbf{f} \quad (6)$$

$$\nabla \cdot \mathbf{v} = 0 \quad (7)$$

where  $\mathbf{v}$  is the velocity vector,  $\partial \mathbf{v} / \partial t$  is Eulerian derivative of the velocity.  $\mathbf{w}$  is the velocity associate to motion of the mesh.  $P$  is the pressure in flow material,  $\mathbf{f}$  the external body force.  $\rho$  is the density of feedstock evaluated by mixtures law:

**Fig. 6.** Description of the modeling in twin-screw mixing chamber and the finite element mesh.

**Table 2**  
Thermal parameters for PP/MWCNT nanocomposites.

	0 wt.%	10 wt.%	20 wt.%	30 wt.%	40 wt.%
Density (g cm <sup>-3</sup> )	0.905	0.82	0.736	0.651	0.567
Specific heat (J kg <sup>-1</sup> K <sup>-1</sup> )	1800	1800.2	1800.4	1800.6	1800.8
Thermal conductivity (W m <sup>-1</sup> kg <sup>-1</sup> )	0.2	300.18	600.16	900.14	1200.12

$$\rho = \Phi \rho_f + (1 - \Phi) \rho_m \quad (8)$$

where  $\Phi$  is volume fraction of MWCNT (corresponding to 10, 20, 30 and 40 wt.%),  $\rho_f$  is the density of pure PP, and  $\rho_m$  is the proper density of MWCNT.

The conversion between weight percentage and volume fraction of the multi-walled carbon nanotubes is rather direct and explicit.

$$\text{wt.}\% = \frac{\rho_m \Phi}{\rho_m \Phi + \rho_f (1 - \Phi)}, \quad \Phi = \frac{\rho_f \text{ wt.}\%}{\rho_f \text{ wt.}\% + \rho_m (1 - \text{wt.}\%)} \quad (9)$$

Key issue of the conversion is the measurement of pure density for multi-walled carbon nanotubes. The helium pycnometer in our laboratory is an effective equipment to achieve the necessary values.

For a generalized non-Newtonian fluid, the stress tensor  $\sigma$  incorporates the pressure ( $p$ ) and extra stress tensor ( $K$ ), defined as

$$\sigma = -pI + 2\mu(\dot{\gamma}, T) \bar{D} \quad (10)$$

where  $\bar{D}$  is the deviatoric strain rate tensor.  $\mu$  is the Carreau–Yasuda viscosity as given in Eq. (3), function of the local shear rate  $\dot{\gamma}$  and the temperature  $T$ .

Evolution of the temperature is governed by energy conservation. It takes the form:

$$\rho C_p \left( \frac{\partial T}{\partial t} + (\mathbf{v} - \mathbf{w}) \cdot \nabla T \right) - \nabla \cdot (k \nabla T) = \dot{q} \quad (11)$$

where  $T$  stands for temperature.  $C_p$  and  $k$  are specific heat and thermal conductivity of the nanocomposite, respectively.  $\dot{q}$  represents source of the heat generated in the flow material. Specific heat of

the nanocomposite can be determined by Hamilton and Crosser model [21]:

$$C_p = C_{pm} \frac{\alpha + (n-1) - (n-1)(1-\beta)\Phi}{\alpha + (n-1) + (1-\beta)\Phi} \quad (12)$$

$$\beta = \frac{C_{pf}}{C_{pm}}, \quad \alpha = \frac{k_f}{k_m} \quad (13)$$

where  $n$  is a shape factor ( $n = 6$  for cylindrical particles),  $\alpha$  and  $\beta$  are the dimensionless coefficients.  $C_{pf}$  and  $C_{pm}$  are the specific heat of MWCNT and matrix,  $k_f$  and  $k_m$  are thermal conductivity of the MWCNT and matrix respectively.

Thermal conductivity  $k$  of the nanocomposite can be determined by the mixture rule reported by Han et al. [22] and Zhou et al. [23].

$$k = \Phi k_f + (1 - \Phi) k_m \quad (14)$$

The values of density, specific heat and thermal conductivity for different PP/MWCNT nanocomposites are reported in Table 2.

#### 4.2. Boundary and initial conditions in simulation

For flow motion of the mixture, no slip condition on the walls of mixing chambers and screws are imposed. The open boundary at inlet of the mixer corresponds to a zero pressure. Between the inner and outer subdomains, the continuity condition for transfer of the loads is respected. Heat flux through inlet of the mixer is prescribed by

$$K \vec{\text{grad}}(T) = h(T - T_{\text{ext}}) \vec{n} \quad \text{on} \quad \partial_4 \Omega \quad (15)$$

The mixer was heated to 200 °C in mixing process. The temperature was measured by a thermocouple. The measurement proved well the temperature at walls of the mixing chamber is the set temperature (200 °C). But temperature of the screws equals 150 °C as they are heated by conduction. The boundary conditions in simulation respect the measured values. The continuity conditions for thermal effect between the inner and outer subdomains, are set to be the equal heat flux on both sides, no source is introduced in the boundaries. The initial conditions are defined to be zero velocity, environment pressure, and environment temperature at 20 °C.

#### 4.3. Rotating frames of the inner subdomains

The modeling and equations for both subdomains  $\Omega_2$  and  $\Omega_3$  are solved in rotating frames  $(O_1, x_1, y_1, z_1)$  and  $(O_2, x_2, y_2, z_2)$ , respectively, as shown in Fig. 6. The motions of rotating frames are described typically by angular velocity  $\theta$  of the primary rotating component. In the present study, the frames rotate with the screws. The mixing chamber is assumed to rotate in the opposite direction, in order to get a rotational boundary condition corresponding to  $-\theta$ . To calculate the rotation, two methods can be used, either matrix algebra or complex number. For each method it rotates the subdomain  $\Omega_2$  clockwise through an angle  $\theta$  and the subdomain  $\Omega_3$  counterclockwise through an angle  $\text{srd} \times \theta$  around the third axis of both moving frames.  $\text{srd}$  is the speed ratio driven.

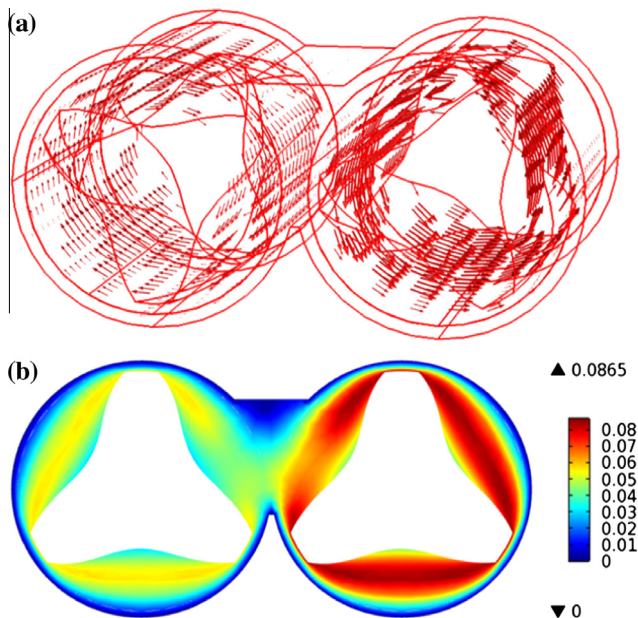


**Fig. 7.** Velocity field in twin-screw mixer (a) expressed by vectors in 3D model and (b) the speed field on a cross section (at  $z = 24$  mm).

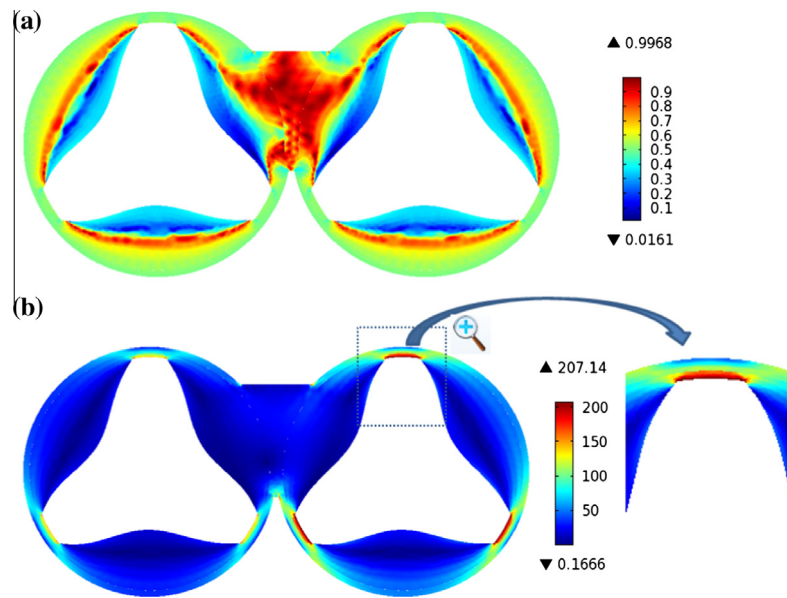


Fig. 8. Results in a cross section of the twin screw mixer ( $z = 24$  mm) after 10 revolutions of the left screw: (a) distribution of the mixing index ( $\lambda_{MI}$ ) and (b) shear rate field.

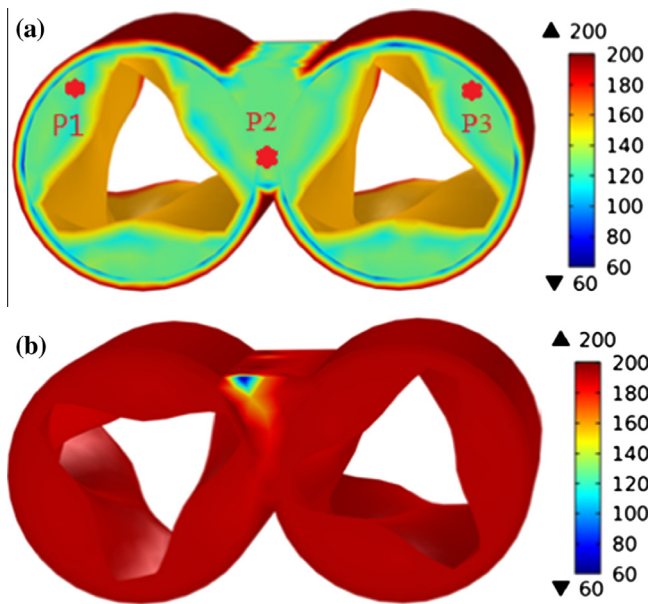


Fig. 9. Temperature field ( $^{\circ}\text{C}$ ) at two time step in twin-screw mixer, imposed temperature  $200^{\circ}\text{C}$ , rotation speed 30 rpm. 3 positions (P1, P2, P3) are shown in (a), where temperature is especially measured for comparison with the numerical results: (a) at  $t = 0$ , (b) at  $t = 90$  s.

#### 4.4. Dispersive mixing characterization

In order to achieve good dispersion, it is necessary that the agglomerates of MWCNT repetitively squeezed. Multiple passes

of the MWCNT nanocomposite through the mixing screws at necessary. For one such a measurement, the flow number  $\lambda_{MI}$  has been used by many authors to define the flow pattern [24,25].  $\lambda_{MI}$  is defined by Eq. (16) in terms of the magnitudes of strain rate tensor  $D$  and vorticity tensor  $\omega$ .

$$\lambda_{MI} = \frac{|D|}{|D| + |\omega|} \quad (16)$$

The flow number varies between 0 and 1. For a flow number 0, the system undergoes purely rotational flow with no effective mixing. A flow number 0.5 denotes simple shear flow, while a value 1.0 denotes a pure elongational flow. In mixing process, whenever the flow number is greater than or equal to 0.7, the system produces elongational flow for dispersion.

#### 4.5. Mixing torque calculation

For driving of the mixing screw, the mixing torque is expressed as:

$$\vec{M} = \int_S (\vec{r} \times \vec{F}) \cdot \vec{n}_z dS \quad (17)$$

where  $\vec{r}$  represents the position vector from axis of the screw to the point and under consideration,  $S$  is the surface of the screw in contact with the nanocomposite of the mixing screw,  $\vec{F}$  is the force on the surface of the screw acted on by the nanocomposite. The force  $\vec{F}$  can be expressed as:

$$\vec{F} = \sigma \cdot \vec{n} \quad (18)$$

where  $\sigma$  is the stress tensor and  $\vec{n}$  is the unit vector normal to surface of the screw.

Table 3  
Temperature values at 3 positions, results of measurement and simulation.

Points Identity	Location		After 10 revolutions		After 70 revolutions	
	X (mm)	Y (mm)	Exp. ( $^{\circ}\text{C}$ )	Num. ( $^{\circ}\text{C}$ )	Exp. ( $^{\circ}\text{C}$ )	Num. ( $^{\circ}\text{C}$ )
P <sub>1</sub>	10	17	168.41	165.33	203.14	199.15
P <sub>2</sub>	25	15	155.52	158.27	202.51	199.46
P <sub>3</sub>	60	20	160.21	162.24	203.21	199.12



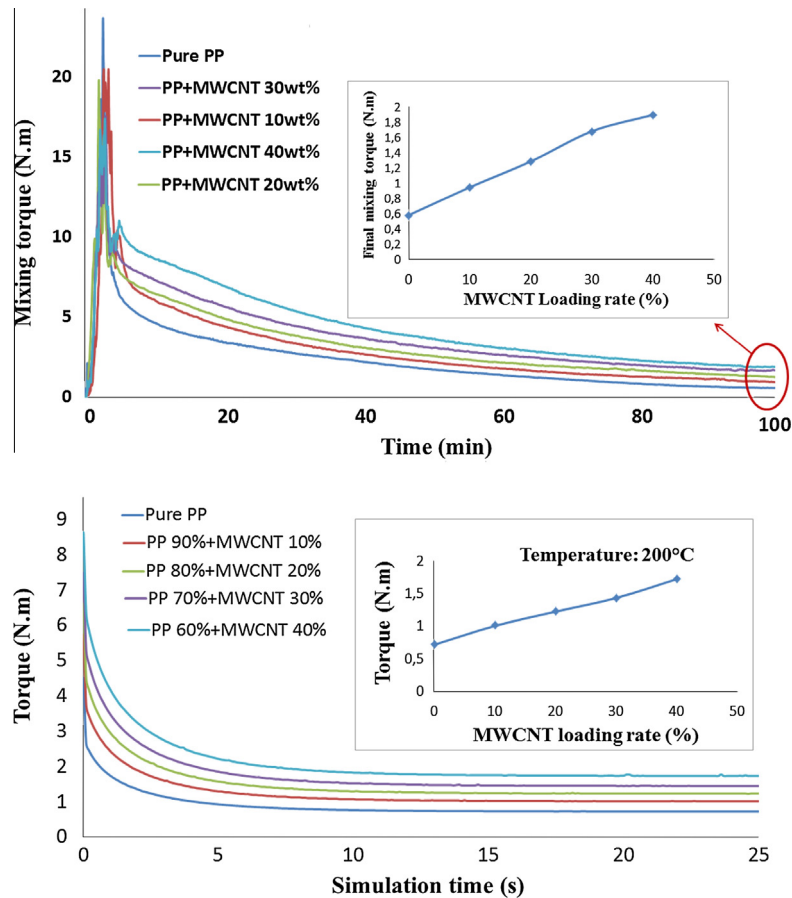


**Fig. 10.** Comparison between the evolutions of mixing torque obtained by measurement (a) and simulation (b), 200 °C and 10 rpm for pure PP and PP/MWCNT nanocomposite (10%, 20%, 30% and 40% in weight).

#### 4.6. 3D numerical simulation of the mixing stage in twin-screw mixers

COMSOL® Multiphysics software is adopted for simulation of the PP/MWCNT flow in co-rotating mixer as it is well adapted for complex physics. The coupling of flow-thermal model has been solved with ALE moving mesh. The mesh consists of 18,177 tetrahedral elements with 90,336 nodes, see Fig. 6. A transient analysis is performed in the actual frames at each time step until  $t = t_f = 25$  s.

### 5. Results and discussions

The discussion is focused on the results of PP/MWCNT nanocomposite with 40 wt.% MWCNT in its mixing stage.

#### 5.1. The flow pattern and velocity vectors

The vectors of velocity in Fig. 7a indicate that the material flows generally along the screw surface, with an additional flow in the gap between two screws in axial direction. Due to the speed ratio (2:3) between two screws, speed of the nanomaterial flow in right subdomain is greater than that in the left subdomain. The maximum speed locates in middle of the space between the right screw and the chamber. The moving wall condition is imposed to the screw, which results in significant shear rate especially in the gap between the screws and mixing chamber. The wall conditions are imposed to be the non slip ones on both the screw surface and mixer chamber inside as seen in Fig. 7b. One can also remark that the speed is reduced in the gap between the screws, caused by the

flow due to counter rotation of the screws. This is observed in experiment through the transparent front wall in mixing phase.

#### 5.2. Dispersive mixing field

The mixing index ( $\lambda_{MI}$ ) and shear rate on a cross section of nanocomposite flow are shown in Fig. 8a and b, respectively. It represents the mixing phase after 10 revolutions of the left screw (which correspond to 15 revolution of the right screw).

It happens the elongational flow in the gap between the screws and the chamber of the mixer, while largest shear rate appears at tips of the screws, too. The elongational flow causes breakup of the agglomerates. Observing together the mixing index, shear rate and the velocity vectors fields shown in Fig. 7, flow of the nanocomposite is spitted, reoriented and folded in the gap between the screws.

#### 5.3. Temperature field in simulation for PP/MWCNT nanocomposite

Evolution of the temperature in nanomaterial during mixing phase is shown in Fig. 9. At beginning, the temperature is about 130 °C. On walls of the frame and screws, the temperature is set to 200 °C and 150 °C, respectively (Fig. 9a). In simulation, temperature of the nanocomposite increases up to 200 °C, corresponding to the imposed mixing temperature (Fig. 9b). It indicates clearly that the mixing temperature is quickly reached, which guarantees the optimal mixing conditions. The influence of heat transfer at the mixer inlet is related in Fig. 9. One can remark a significant

variation of the temperature at middle of the cavity, where the temperature is practically equal to the PP melting temperature.

#### 5.4. Comparison between the results of experiment and simulation

The temperature values at 3 different locations ( $P_1$ ,  $P_2$ ,  $P_3$ ) in twin screw mixer shown in Fig. 9, have been summarized in Table 3. It exhibits the correlation between the measured values and the numerical results for mixing of the PP/MWCNT 40 wt.%.

#### 5.5. Mixing torque as the result of simulation

The evolutions of mixing torque in simulation, and the ones measured by experiments, are shown in Fig. 10. The torque increases with increase of the MWCNT ratio, because of the increase of shear viscosity for PP/MWCNT nanocomposites. The mixing torque decreases gradually to a limit value as viscosity of the polymer melts varies with temperature according to Arrhenius law (5). Agreement is obtained between the mixing torques in simulation and experiment.

## 6. Conclusions

The analyses on physical modeling and 3D simulation of PP and PP/MWCNT viscous flow, based on identification of the material behaviors, have been realized by FEM. The work investigated first the viscous behaviors of PP and PP/MWCNT nanocomposites at 4 selected temperatures (180, 200, 220 and 240 °C). Their rheological properties have been measured in the range  $[10^{-10}^4]$  by capillary rheometer. The effect of MWCNT ratio on shear viscosity is significant. Shear viscosity increases for all range of the shear rate, when MWCNT volume fraction increases. These rheological behaviors are used to set up the constitutive models for simulation, based on the extension of Carreau law for thermal effects. Parameters of the model have been identified for pure PP and different PP/MWCNT nanocomposites. Good correlation can be observed between the experimental data and Carreau–Yasuda behavior law.

Then modeling and simulation of the PP/MWCNT nanocomposite flow in twin screw mixer has been realized, with identified flow models implemented in COMSOL© software. The results of 3D simulation are compared with the experimental ones for the mixing torque, mixing index and temperature field. Comparison between the mixing torques obtained by simulations and experiments proved validity of the rheological flow model and the simulation results. The proper correlation is observed between the measured temperature and the ones in simulation.

## Acknowledgements

The research has been supported by the FUI project named “NewPIM”. The authors acknowledge the project sponsors for funding this research through the FEMTO-ST Institute.

## References

- [1] Iijima S. Helical microtubes of graphitic carbon. *Nature* 1991;354:56–8.
- [2] Pötschke P, Bhattacharyya A, Janke A, Goering H. Melt mixing of polycarbonate/multi-wall carbon nanotube composites. *J Compos Interfaces* 2003;10:389–404.
- [3] Wei C, Cho K, Srivastava D. Tensile strength of carbon nanotubes under realistic temperature and strain rate. *J Phys Rev B* 2003;67:11540–7.
- [4] Dresselhaus MS, Dresselhaus G, Eklund PC. *Science of fullerenes and carbon nanotubes*. J. Academic Press; 1996.
- [5] Funck A, Kaminsky W. Polypropylene carbon nanotube composites by in situ – polymerization. *J Compos Sci Technol* 2008;67:906–15.
- [6] Demczyk BG, Wang YM, Cumings J, Hetman M, Ham W, Zettl A. Direct mechanical measurement of the tensile strength and elastic modulus of multiwalled carbon nanotubes. *J Mater Sci Eng A* 2002;334:173–8.
- [7] Shaffer MSP, Windle AH. Fabrication and characterization of carbon nanotube/poly(vinyl alcohol) composites. *Adv Mater*, J Adv Mater 1999;11:937–41.
- [8] Prashantha K, Soulestin J, Lacrampe MF, Krawczaka P, Dupin G, Claesb M. Masterbatch-based multi-walled carbon nanotube filled polypropylene nanocomposites: assessment of rheological and mechanical properties. *Compos Sci Technol* 2009;69:1756–63.
- [9] Lee SH, Kim M, Sung Ho Kim, Youn JR. Rheological and electrical properties of polypropylene/MWCNT composites prepared with MWCNT masterbatch chips. *Eur Polymer J* 2008;44:1620–30.
- [10] Zhan WD, Shen L, Phang IY, Liu T. Carbon nanotubes reinforced nylon-6 composite prepared by simple melt-compounding. *Macromolecules* 2004;37:256–9.
- [11] Thiébaud F, Gelin J-C. Characterization of rheological behaviors of polypropylene/carbon nanotubes composites and modeling their flow in a twin-screw mixer. *J Compos Sci Technol* 2010;70:647–56.
- [12] Zhou X, Xie X, Zeng F, Li RK-Y, Mai Y-W. Properties of polypropylene/carbon nanotube composites compatibilized by maleic anhydride grafted SEBS. *J Key Eng Mater* 2006;312:223–8.
- [13] Cross MM. Rheology of non-Newtonian fluids: a new flow equation for pseudoplastic systems. *J Colloid Sci* 1965;20:417–37.
- [14] Bourgeat A, Marusic-Paloka E. Non-linear effects for flow in periodically constricted channel caused by high injection rate. *Math Models Methods Appl Sci* 1998;8:1–25.
- [15] Djoudi H, GELIN J-C, Barriere T. Characterization of rheological behavior and numerical results concerning mixing process in Brabender twin-screw mixer of polymers and loaded polymers. In: ICOMM 2012 conference, Northwestern University, USA; 12–14 March 2012.
- [16] Kong X, Barrière T, Gelin JC. Manufacturing of stainless steel and cu bi-material micro-components with micro-powder injection molding process. *J Mater Process Technol* 2012;212:2173–82.
- [17] Kelarakis A, Yoon K, Sics I, Somani RH, Chen X, Hsiao BS. Shear-induced orientation and structure development in isotactic polypropylene melt containing modified carbon nanofibers. *J Macromol Sci* 2006;45:247–61.
- [18] Gu SY, Ren J, Wang QF. Rheology of poly(propylene)/clay nanocomposites. *J Appl Polym Sci* 2004;91:2427–34.
- [19] Akdogan H, McHugh TH. Twin screw extrusion of peach puree: rheological properties and product characteristics. *J Food Process Pres* 1999;23:285–305.
- [20] Fasina OO, Hallman CHM, Clements C. Predicting temperature-dependence viscosity of vegetable oils from fatty acid composition. *JAOCS* 2006;83:899–903.
- [21] Hamilton RL, Crosser OK. Thermal conductivity of heterogeneous two component systems. *Ind Eng Chem Fundam* 1962;1:1–187.
- [22] Han Z, Fina DA. Thermal conductivity of carbon nanotubes and their polymer nanocomposites. *J Prog Polym Sci* 2012;36:914–44.
- [23] Zhou H, Zhang S, Yang M. The effect of heat transfer passages on the effective thermal conductivity of high filler loading composite materials. *J Compos Sci Technol* 2007;67:1035–40.
- [24] Manas-Zloczower I et al. Dispersive and distributive mixing characterization in extrusion equipment. *J ANTEC Proc* 2001:220–5.
- [25] Cong L, Gupta M. Simulation of distributive and dispersive mixing in a co-rotating twin-screw extruder. *J Soc Plast Eng Annu Tech (ANTEC)* 2008;54:300–4.